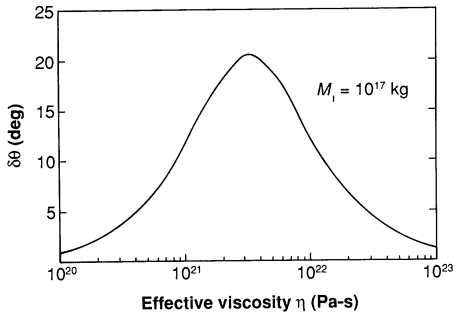

Fig. 1. Change in obliquity $\delta\Theta$ as a function of effective viscosity η for a cap radius of 10° and $M_i = 10^{17}$ kg. The total change in cap mass over one cycle is $2M_i$. Larger or smaller changes in mass shift the curve proportionally up or down. The instantaneous obliquity today is 25.2°, which is coincidentally near the present average of 24.4°.

planet

$$\Delta J_2^0 = -M_i(\cos\xi \cos\Psi)/M \qquad (10)$$

Viking spacecraft measurements indicate that $\sim 3 \times 10^{17}$ kg of CO_2 is flushed every 10^5 years from the megaregolith (*7, 10*). Such a vast reservoir of oxygen is needed to explain the lack of enrichment of ^{18}O relative to ^{16}O, as would be expected from exospheric escape. I will adopt an estimate of $M_i = 10^{17}$ kg, with $\Psi = 10°$ (*7*).

The effective viscosity of Mars' mantle is not known; the change in obliquity for various viscosities based on Eqs. 8 through 10 is shown in Fig. 1. For comparison, the effective viscosity of Earth's upper mantle is about 10^{21} Pa-s (*11*). Values only slightly higher than Earth's account for nearly the entire obliquity of the red planet.

Mars is less active tectonically than Earth, so that one might expect a cooler interior and a higher viscosity. On the other hand, experimental studies (*12*) indicate that the effective viscosity of Mars may be 4×10^{20} Pa-s or less (for tectonic loads on the order of 100 bars, rather than the more modest $\sim$1 bar for the massive caps). Thus the range of viscosities shown in Fig. 1 does not appear to be unreasonable, and the axial tilt of Mars may have changed significantly over the age of the solar system. This could have important implications for the paleoclimate of this planet.

REFERENCES AND NOTES

1. B. C. Murray, W. R. Ward, S. C. Yeung, *Science* **180**, 638 (1973); W. R. Ward, *ibid.* **181**, 260 (1973).
2. W. R. Ward, *J. Geophys. Res.* **79**, 3375 (1974).
3. ———, *ibid.* **84**, 237 (1979).
4. ———, J. A. Burns, O. B. Toon, *ibid.*, p. 243.
5. B. G. Bills, paper presented at the annual spring meeting of the American Geophysical Union, Baltimore, MD, 7 to 12 May 1989. Bills has the average obliquity having a value as high as 40° only tens of millions of years ago. His model depends on a value of the moment of inertia that is substantially smaller than the accepted value. For a rebuttal to Bills' argument, see W. M. Kaula, N. H. Sleep, R. J. Phillips, *Geophys. Res. Lett.* **16**, 1333 (1989); for a reply, see B. G. Bills, *ibid.*, p. 1337.
6. D. P. Rubincam, in preparation.
7. F. P. Fanale, J. R. Salvail, W. B. Banerdt, R. S. Saunders, *Icarus* **50**, 381 (1982); L. M. François, J. C. G. Walker, W. R. Kuhn, *Eos* **70**, 388 (1989) (abstract).
8. R. B. Leighton and B. C. Murray, *Science* **153**, 136 (1966); W. R. Ward, B. C. Murray, M. C. Malin, *J. Geophys. Res.* **79**, 3387 (1974). The time delay of the cap is about 250 years, which is small compared to the 127,000-year period of the obliquity cycle.
9. Equations 9 and 10 are perhaps most easily derived from pages 655 and 656 of W. R. Peltier, *Rev. Geophys. Space Phys.* **12**, 649 (1974). Peltier's derivation must be modified to include the gravitational attraction of the load, which he intentionally omits. This requires the extra term $3L_n/(2n + 1)$ in his equation 35 where L_n is the spherical harmonic coefficient of the load. The calculation of ΔJ_2 assumes that the CO_2 is removed uniformly all over the regolith and deposited evenly on the cap. D. P. Rubincam [*J. Geophys. Res.* **89**, 1077 (1984)] considers a similar case for the oceans and the Laurentide ice sheet on Earth, but with the more sophisticated layered model of P. Wu and W. R. Peltier [*Geophys. J. R. Astron. Soc.* **70**, 435 (1982)]. The simple model adopted here can only give orders of magnitude for viscosities.
10. A. O. Nier, M. B. McElroy, Y. L. Yung, *Science* **194**, 68 (1976); M. B. McElroy, Y. L. Yung, A. O. Nier, *ibid.*, p. 70.
11. See, for example, J. X. Mitrovica and W. R. Peltier [*J. Geophys. Res.* **94**, 13,651 (1989)] and R. Sabadini, D. A. Yuen, and P. Gasperini [*ibid.* **93**, 437 (1988)] and references therein.
12. W. B. Banerdt, R. J. Phillips, N. H. Sleep, R. S. Saunders, *ibid.* **87**, 9723 (1982). Their estimate of viscosity is based on experiments with olivine crystals by D. L. Kohlstedt and C. Goetze [*ibid.* **79**, 2045 (1974)].

13. I thank S. Blackwell for programming support and two anonymous referees for their corrections and criticisms. T. Clark's suggestion of looking for seasonal changes in J_2 with the Mars Observer ultimately led to the present investigation.

1 December 1989; accepted 5 March 1990

Spatial Variation of Ozone Depletion Rates in the Springtime Antarctic Polar Vortex

YUK L. YUNG, MARK ALLEN, DAVID CRISP, RICHARD W. ZUREK, STANLEY P. SANDER

An area-mapping technique, designed to filter out synoptic perturbations of the Antarctic polar vortex such as distortion or displacement away from the pole, was applied to the Nimbus-7 TOMS (Total Ozone Mapping Spectrometer) data. This procedure reveals the detailed morphology of the temporal evolution of column O_3. The results for the austral spring of 1987 suggest the existence of a relatively stable collar region enclosing an interior that is undergoing large variations. There is tentative evidence for quasi-periodic (15 to 20 days) O_3 fluctuations in the collar and for upwelling of tropospheric air in late spring. A simplified photochemical model of O_3 loss and the temporal evolution of the area-mapped polar O_3 are used to constrain the chlorine monoxide (ClO) concentrations in the springtime Antarctic vortex. The concentrations required to account for the observed loss of O_3 are higher than those previously reported by Anderson *et al.* but are comparable to their recently revised values. However, the O_3 loss rates could be larger than deduced here because of underestimates of total O_3 by TOMS near the terminator. This uncertainty, together with the uncertainties associated with measurements acquired during the Airborne Antarctic Ozone Experiment, suggests that in early spring, closer to the vortex center, there may be even larger ClO concentrations than have yet been detected.

MAN-MADE HALOCARBONS HAVE been generally recognized as the cause of enhanced springtime O_3 depletion in the Antarctic stratosphere (*1–7*). However, the detailed description of O_3 loss rates in the "O_3 hole" needed for testing the theories quantitatively is not known. The most comprehensive global and temporal O_3 data set is the TOMS data obtained by the Nimbus-7 spacecraft since 1978 (*2, 8*). This instrument derives high-quality total column O_3 (precision $\sim$1%) from backscattered sunlight in several ultraviolet channels. Daily data sets are available for 1979 through 1989 with latitude and longitude resolutions of 2° and 5°, respectively, covering the whole globe except for the unilluminated winter poles, where data collection is impossible. It is difficult to extract from these data information on the spatial dependence of the O_3 loss rate in spring within the polar vortex for two reasons. First, the center of the O_3 hole (as defined by the minimum O_3 isopleth) does not stay fixed at the South Pole. It may wander off the pole by as much as 10° in a few days. Second, the

Y. L. Yung, Division of Geological and Planetary Sciences, California Institute of Technology, Pasadena, CA 91125.
M. Allen and D. Crisp, Jet Propulsion Laboratory, California Institute of Technology, Pasadena, CA 91109, and Division of Geological and Planetary Sciences, California Institute of Technology, Pasadena, CA 91125.
R. W. Zurek and S. P. Sander, Jet Propulsion Laboratory, California Institute of Technology, Pasadena, CA 91109.

O_3 isopleths are not parallel to the latitude circles. They can become distorted, elongated, twisted, and occasionally broken up in a very short period in response to wave activity. Because of these fundamental difficulties, no quantitative information has been derived on the relative rates of O_3 loss from the center of the vortex to the collar.

We have analyzed the TOMS data in a way that reduces the local and temporal variability by using the horizontal projection of the area enclosed inside an O_3 contour as the radial coordinate. This method is similar to that used in area mapping of Ertel's potential vorticity on an isentropic surface (*9*). Let $\Omega(\theta, \phi, t)$ be the observed column abundance of O_3, as a function of latitude (θ), longitude (ϕ), and time (t). A contour line is defined by the isopleth $\Omega(\theta, \phi, t) = \Omega^*$. The area $A(t, \Omega^*)$ is defined as the total projected area enclosed by the contour $\Omega = \Omega^*$,

$$A(t, \Omega^*) = \int_{\Omega<\Omega^*} dA(t, \Omega) \qquad (1)$$

where $dA(t, \Omega)$ is the horizontal projection of an area element. This definition is most useful when Ω decreases monotonically (but not necessarily uniformly) toward the center of the vortex. When this condition is not satisfied (for example, when an isopleth encloses two distinct patches of area), Eq. 1 is still well defined mathematically, but its physical interpretation becomes obscure. Inspection of the TOMS data atlas (*10*) confirms that the isopleths typically increase monotonically from the center of the vortex to close to the collar but generally not beyond the collar region. If the distribution of O_3 were zonally symmetric around the pole, then the isopleth Ω^* would coincide with the latitude circle θ^*. In this case, $A(t, \Omega^*)$ would simply be the total projected area southward of θ^*,

$$A(t, \Omega^*) = A(t, \theta^*) = 2\pi R^2[1 - \cos(90° + \theta^*)] \qquad (2)$$

where R is the planetary radius, and θ^* is the latitude defined to be 0° at the equator and −90° at the South Pole. When the isopleths are not azimuthally symmetric, Eq. 2 can still be used to define the equivalent latitude θ_E,

$$A(t, \Omega^*) = 2\pi R^2[1 - \cos(90° + \theta_E)] \qquad (3)$$

The equivalent latitude represents the latitude at which a zonally symmetric contour Ω^* would lie if it enclosed an area $A(t, \Omega^*)$. The entire Southern Hemisphere has an area $A = 2\pi R^2$, and we will adopt this quantity as a convenient unit. Another important physical quantity is the total area-integrated

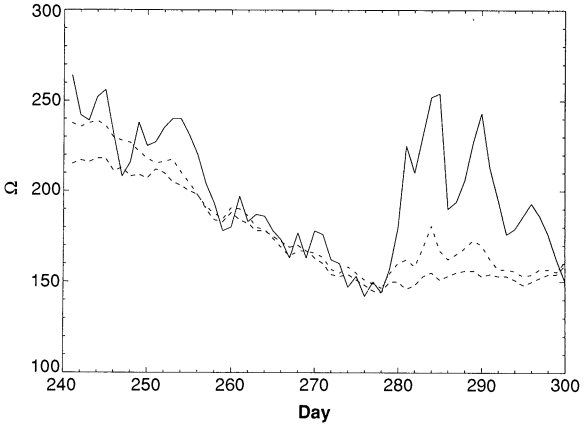

Fig. 1. Column abundances of O_3 $\Omega(t)$, in Dobson units (1 DU = 2.69×10^{16} molecules cm^{-2}), plotted against day number in 1987. Solid line, McMurdo (78°S, 166°E); dashed line, area-mapped data with equivalent latitude (as defined by Eq. 3), $\theta_E = -78°$; dash-dot line, zonally averaged data for latitude $\theta = -78°$. Days 240, 260, 280, and 300 correspond, respectively, to 28 August, 17 September, 7 October, and 27 October. All data were taken by TOMS (*8*).

O_3 within an area A

$$\Sigma(t, A) = \int_{\sigma<A} \Omega(t, \sigma) d\sigma \qquad (4)$$

The natural unit for Σ is the Area-Dobson unit (1 ADU = $2\pi R^2 \times 1$ DU = 6.88×10^{34} molecules; Σ = 600 ADU for a hypothetical terrestrial atmosphere containing 300 DU of O_3 mixed uniformly over the globe).

Figure 1 shows a comparison between TOMS measurements over McMurdo (78°S, 166°E) from day 240 (28 August) to day 300 (27 October) and zonally averaged data for latitude $\theta = -78°$, and area-mapped data for $A = 0.0219$ ($\times 2\pi R^2$, corresponding to $\theta_E = -78°$). Both zonal averaging and area mapping tend to filter out the synoptic perturbations, but the area-mapped quantities also appear to remove variations resulting from the displacement of the polar vortex away from the pole. Because of this, the area-mapped data vary more smoothly than the zonal average (*11*). For example, the large secondary maximum in the original McMurdo data after day 280 is primarily caused by the 10° displacement of the vortex toward Punta Arenas (53°S, 71°W). [This displacement is most easily seen in the Nimbus-7 TOMS data atlas (*10*).] Zonal averaging failed to remove this type of motion completely, but area mapping did. Thus, area mapping provides a more reliable measure of the time evolution of O_3 in the vortex than zonal averaging. This method is particularly valuable when one is making quantitative comparisons between data and theory for O_3 change (*12*).

The area-mapping technique is most useful for revealing the regional morphology of O_3 temporal evolution inside the vortex. For example, the analysis of O_3 for the polar region in spring shows (Fig. 2) the rapid depletion of O_3 from day 240 to day 278 in the vortex. Figure 3 presents a more detailed description of O_3 change over this period. It illustrates the existence of an extremely stable collar region always seen in the vicinity of $\theta_E = 62°S$. Inside the vortex the O_3 change increases toward the center. This trend is more readily seen if we differentiate Ω with respect to time (*13, 14*).

Figure 4 presents O_3 destruction rates ($\partial\Omega/\partial t$). The results also show two distinct regimes. Changes in Ω equatorward of $\theta_E = -62°$ are oscillatory, with periods of ≤20 days, and are due most likely to the action of planetary waves outside the polar vortex. The region of dynamical influence extends poleward toward the end of September and may dominate the O_3 change in October, long before the final warming in November. The rate of O_3 depletion poleward of $\theta_E = -62°$ during September, however, may be due solely to chemical destruction. [This area, sampled during the Airborne

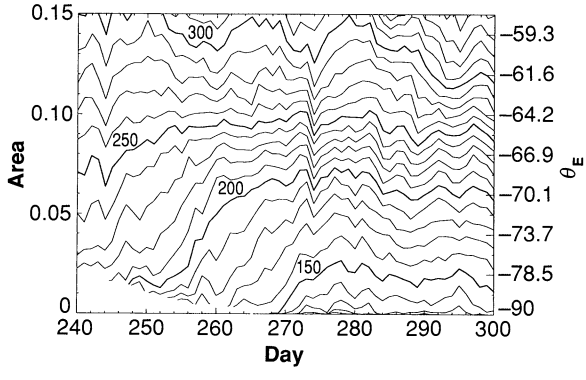

Fig. 2. Contours of column O_3 abundances $\Omega(t)$ in Dobson units plotted against enclosed area $A(t, \Omega)$ in units of $2\pi R^2$ from day 240 to day 300. The blank space in the lower left corner is caused by lack of data. Positive slopes indicate O_3 decreases, negative slopes indicate O_3 increases. The complete TOMS data for this period without smoothing are shown. The spacing between the contours is 10 DU. The equivalent latitude θ_E is shown on the right scale.

Antarctic Ozone Experiment (AAOE), was identified as a chemically perturbed region.] The rate of O_3 depletion was generally largest close to the pole and remained high, ~2 to 3 DU day^{-1}, from day 245 (2 September) to day 274 (1 October).

An examination of $\Sigma(t, A)$, (Eq. 4), shows additional features. At $A = 0.15$ ($\times 2\pi R^2$, $\theta_E = -58°$), Σ was equal to 35 ADU on day 240 and steadily decreased to 31 ADU on day 280. Because the area defined by $A = 0.15$ ($\times 2\pi R^2$) includes the collar as well as the vortex, we conclude that the sum of O_3 in these two regions decreased during this period. This is an unambiguous signature of the loss of O_3 by chemical destruction. After day 280 there was a steady increase of Σ to about 33 ADU at day 300, consistent with the influx of O_3-rich air from lower latitudes.

There was a curious rate of O_3 loss of about 1 DU day^{-1} near day 290. The contour for −0.5 DU day^{-1} (not shown in Fig. 4) extends from the collar to the pole. The extent of this decrease cannot be attributed to chemical destruction of O_3 because the catalytic schemes have by this time become ineffective (*15*). The nearly constant values of Σ around day 290 at the collar region ($A = 0.12 \times 2\pi R^2$, $\theta_E = -62°$) suggest instead that the rapid decrease represents redistribution rather than chemical destruction. This could be accomplished by upwelling of tropospheric air followed by displacement of air from the center of the vortex (at about 18 km) toward the collar as first proposed by Tung *et al.* (*16*) and Mahlman and Fels (*17*).

How do we relate the observed O_3 depletion rates shown in Fig. 4 to current theories? The effect of all important known catalytic schemes (*3*) and dynamics (*16, 17*) may be summarized by the following expression,

$$\frac{\partial \Omega}{\partial t} = -2 \int_0^\infty [\mathrm{ClO}](k_1[\mathrm{ClO}] + k_2[\mathrm{BrO}] + k_3[\mathrm{HO_2}])\, dz - \nabla \cdot \mathbf{F} \quad (5)$$

where $[x]$ denotes the concentration of species x; k_1, k_2, and k_3 are the appropriate rate coefficients (*3, 5, 7*); and $\mathbf{F}$ is the vertically integrated horizontal flux of O_3. The integral in Eq. 5 is dominated by contributions from the lower stratosphere (altitude $z \approx 18$ km). On the basis of the modeling of O_3 loss at McMurdo by Sander *et al.* (*7*), the relative contributions of the ClO, BrO, and HO_2 cycles to O_3 destruction are 70%, 23%, and 7%, respectively. Because all catalytic schemes are driven by photolysis, the number of sunlight hours per day, S, must be accurately computed (*18*). We can relate the derived O_3 depletion rates to ClO concentrations if we ignore the dynamical term in Eq. 5. This can be justified because our area-mapping technique has filtered out most of the synoptic fluctuations. Using the simple photochemical model of Sander *et al.* (*7, 19*), we deduced the volume mixing ratios of ClO at 18 km in the vortex ($A = 0 - 0.12\pi R^2$) for days 240 through 280 (Fig. 5). The general trends of ClO—higher values toward the center, values increasing from day 240 to day 255—are consistent with those observed in the AAOE aircraft study (*5*) from day 232 (20 August) to day 265 (22 September). The decline of ClO toward day 280 is also consistent with ground-based observations of OClO from McMurdo (*15*). At about day 255, ClO concentrations reached a peak value of 1.6×10^{-9}, which is considerably higher than the maximum of 1.1×10^{-9} observed by Anderson *et al.* (*5*) on day 252 (9 September) at 18.5 km, 72°S, but is close to their revised value of 1.4×10^{-9} (*20*). Concentrations of ClO as high as 1.7×10^{-9} have been reported as a result of microwave experiments (*21*) during this period (days 263 through 267).

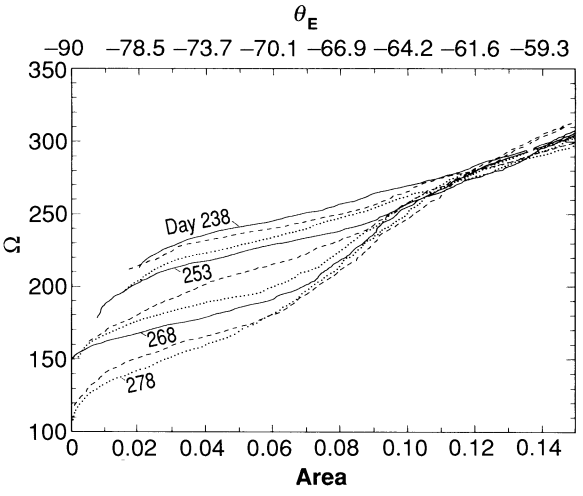

Fig. 3. Column O_3 abundances $\Omega(t)$ in Dobson units plotted against enclosed area $A(t, \Omega)$ in units of $2\pi R^2$ for days 238 to 278 in steps of 5 days. The equivalent latitude θ_E is shown on the upper scale.

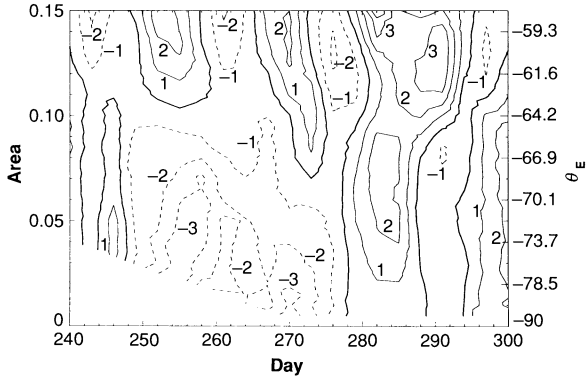

Fig. 4. Contours of the time rate of change of column O_3 ($\partial\Omega/\partial t$), in Dobson units per day, plotted against enclosed area $A(t, \Omega)$ from day 240 to day 300. The dashed lines, heavy lines, and full lines denote negative, zero, and positives rates, respectively. Ozone losses in the vortex were limited by the number of hours of sunlight in early spring, and later by the intrusion of outside air. The time derivative is obtained by differentiating the area-mapped TOMS data presented in Fig. 2 after a 9-day weighted averaging, as described in the text (*13, 14*). The equivalent latitude θ_E is shown on the right scale.

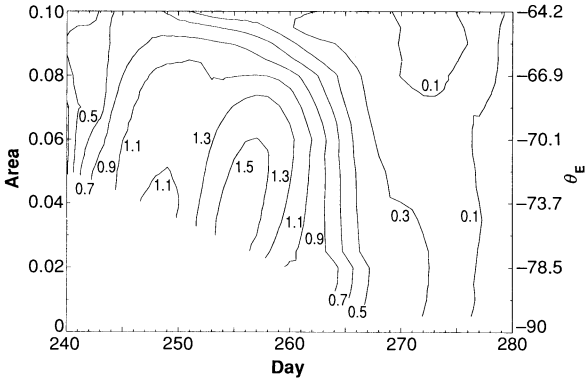

Fig. 5. Contours of ClO concentrations at 18 km in parts per billion by volume ($\times 10^{-9}$) for area = 0 to 0.1 (in units of $2\pi R^2$) and days 240 through 280, derived from Fig. 4 and Eq. 5 without dynamics. The vertical and horizontal scales are different from those in Figs. 2 and 4.

The ClO amounts derived here are sensitive to systematic errors in the retrieved column O_3 amounts (*22*). It has been suggested that TOMS may underestimate O_3 near the terminator. If so, the O_3 loss in the vortex during September—and thus the ClO concentrations—could be greater than computed here. This error implies that ClO concentrations near the center of the O_3 hole were greater than the values that have yet been observed at the more equatorward (equivalent) latitudes reached by the AAOE aircraft.

REFERENCES AND NOTES

1. J. C. Farman, B. G. Gardiner, J. D. Shanklin, *Nature* **315**, 207 (1985).
2. The discovery (*1*) was confirmed by R. S. Stolarski *et al.*, *ibid.* **322**, 808 (1986), using TOMS satellite data.
3. S. Solomon, R. R. Garcia, F. S. Rowland, D. J. Wuebbles, *ibid.* **321**, 755 (1986); M. B. McElroy, R. J. Salawitch, S. C. Wofsy, J. A. Logan, *ibid.*, p. 759; L. T. Molina and M. J. Molina, *J. Phys. Chem.* **91**, 433 (1986).
4. The results of the AAOE are summarized in R. Watson, B. Toon, A. Tuck, Eds., *J. Geophys. Res.* **94**, 11179 (1989); *ibid.*, p. 16437.
5. J. G. Anderson *et al.*, *ibid.*, p. 11465; *ibid.*, p. 11480.
6. J. W. Barrett *et al.*, *Nature* **336**, 455 (1988).
7. S. P. Sander, R. R. Friedl, Y. L. Yung, *Science* **245**, 1095 (1989).
8. R. S. Stolarski and M. R. Schoeberl, *Geophys. Res. Lett.* **13**, 1210 (1986); M. R. Schoeberl, A. J. Krueger, P. A. Newman, *ibid.*, p. 1217.
9. The idea of area mapping of Ertel's potential vorticity on an isentropic surface was first suggested by M. E. McIntyre and T. N. Palmer [*J. Atmos. Terr. Phys.* **46**, 825 (1984)] and fruitfully used by N. Butchart and E. E. Remsberg [*J. Atmos. Sci.* **43**, 1319 (1986)] for studying the northern polar vortex. We have not used Ertel's potential vorticity because of the lack of high-quality dynamical data. Instead we used column O_3, Ω, as a proxy for a conservative tracer.
10. A. J. Krueger *et al.*, *The 1987 Airborne Antarctic Ozone Experiment* (NASA Ref. Publ. 1201, National Aeronautics and Space Administration, Washington, DC, 1988).
11. The difference between the zonal mean O_3 and the area-mapped O_3 can be used as a measure of the effective displacement of the vortex off the pole.
12. For instance, the original McMurdo data show that, from day 240 to day 278, O_3 has apparently decreased by about 120 DU. The area-mapped data indicate that the loss at $\theta_E = -78°$ is only about 70 DU. The remaining 50 DU is caused by displacements of the vortex center. This difference can be significant in a comparison of data and theory. Not only is the loss of 70 DU during this period more compatible with existing chemical theories, but also the shape of the loss profile—slower rate in the early period (when the number of sunlight hours is small) and faster rate later (when the day becomes longer)—is more consistent with these theories (*5*, *7*). The model of Sander *et al.* (*7*) can account for the O_3 loss rates at $\theta_E = -78°$, whereas it has difficulties with the original McMurdo data.
13. We first performed a 9-day weighted averaging of the data to get rid of the daily fluctuations. The relative weighting for the central date is 1 and is 0.8, 0.6, 0.4, and 0.2, respectively, for points ±1, ±2, ±3, and ±4 days away from the central date. A comparison of the original and smoothed data indicates that all the large-scale features of interest are preserved in the smoothing. We have also tried filtering with boxcar windows of 3, 5, 7, and 9 days. The essential features are preserved.
14. The differentiation is carried out by differencing the smoothed data points separated by 1 day. Because of the smoothing described in (*13*), the derived $\partial\Omega/\partial t$ represents O_3 losses averaged over several days.
15. It is generally accepted that the catalytic mechanisms for destroying O_3 are ineffective by this time. S. Solomon *et al.*, *J. Geophys. Res.* **94**, 11393 (1989); R. W. Sanders *et al.*, *ibid.*, p. 11381; C. B. Farmer *et al.*, *Nature* **329**, 126 (1987).
16. K. K. Tung, M. K. W. Ko, J. M. Rodriguez, N. D. Sze, *Nature* **333**, 811 (1986).
17. J. D. Mahlman and S. B. Fels, *Geophys. Res. Lett.* **13**, 1316 (1986).
18. At $z = 18$ km on day 255 (12 September), $S = 12$ hours at all latitudes. Before this date $S < 12$ hours and after this date $S > 12$ hours. The pole at 18 km remains in the shadow before day 250 (7 September) and starts to receive more than 20 hours of sunlight per day after day 260 (17 September). S can be readily computed as a function of latitude, altitude, and time. However, we consider the computation of a static S based on geometry and solar illumination alone as unrealistic, because each parcel of air moves around the pole and makes large excursions across latitude circles. Thus, the correct S must reflect the trajectory history of any air parcel. Because the O_3 isopleths are approximately the trajectories of air parcels in the vortex, we can derive an approximate trajectory-averaged number of sunlight hours per day, $\bar{S}$, by performing the appropriate weighting around each O_3 contour. The general behavior of $\bar{S}$ is consistent with excursions of the vortex off the pole; thus, the number of hours of exposure to sunlight in early spring increased relative to the zonal mean value.
19. We used the model of Sander *et al.* (*7*) without the higher chlorine oxides and with the effective length of the day $\bar{S}$ computed in (*18*). We adopted the vertical profile of ClO obtained by Barrett *et al.* (*6*). On day 260, ClO = 1.1 ppbv at 18 km, $\bar{S} = 15$ hours at McMurdo ($A = 0.0219 \times 2\pi R^2$, $\theta_E = -78°$), $\partial\Omega/\partial t = -2.5$ DU per day. We deduced all other values of ClO at 18 km by inverting Eq. 5 without the dynamical term and holding the concentrations of BrO and HO_2 fixed as in (*7*).
20. W. H. Brune, D. W. Toohey, J. G. Anderson, *Eos* **70**, 1040 (1989).
21. R. L. de Zafra *et al.*, *J. Geophys. Res.* **94**, 11423 (1989).
22. It is known that TOMS measurements tend to underestimate total column O_3 abundances by 20 to 40 DU near the terminator. This error implies that the actual initial O_3 abundances near the vortex center are higher than the values reported here. Hence the loss rates would be higher also.

23. We are grateful to R. Stolarski for providing TOMS data before publication and to P. Newman for sending us potential vorticity data. We thank K. K. Tung, R. Friedl, J. Rodriguez, M. Schoeberl, and R. L. Shia for illuminating discussions, S. Solomon for critical comments on systematic errors of TOMS data, and X.-L. Zhu for plotting all the graphs in this report. Part of the research described in this paper was carried out by the Jet Propulsion Laboratory, under contract with the National Aeronautics and Space Administration, and was also supported by NASA grant NAGW-413 to the California Institute of Technology. Contribution number 4783 from the Division of Geological and Planetary Sciences, California Institute of Technology.

24 October 1989; accepted 22 February 1990

A Genetic Test of the Natal Homing Versus Social Facilitation Models for Green Turtle Migration

ANNE B. MEYLAN, BRIAN W. BOWEN, JOHN C. AVISE

Female green turtles exhibit strong nest-site fidelity as adults, but whether the nesting beach is the natal site is not known. Under the natal homing hypothesis, females return to their natal beach to nest, whereas under the social facilitation model, virgin females follow experienced breeders to nesting beaches and after a "favorable" nesting experience, fix on that site for future nestings. Differences shown in mitochondrial DNA genotype frequency among green turtle colonies in the Caribbean Sea and Atlantic Ocean are consistent with natal homing expectations and indicate that social facilitation to nonnatal sites is rare.

MARINE TURTLES OFTEN USE nesting beaches that are hundreds or even thousands of kilometers removed from their foraging grounds. The hypothesis that marine turtles return to nest on their natal beach (perhaps guided in part by olfaction) (*1*) is derived primarily from the strong nest-site fidelity of adult females, as revealed by repeated capture of tagged individuals on the same beach in successive nesting seasons (*2*–*7*). Despite the fundamental importance of this possibility to an understanding of turtle life histories, the natal homing hypothesis remains unproven. The main obstacle to testing it has been the lack of a physical tag that persists on a turtle for the estimated 30 or more years that elapse between hatching and sexual maturation (*8*). Colonial nesting and nest-site fidelity are known to be especially well developed in the green turtle (*Chelonia mydas*) (*2*, *3*, *4*, *7*); only in rare instances (*9*, *10*) have marked adult females been observed at a nesting beach other than the one at which they were originally tagged.

Hendrickson (*11*) and Owens *et al.* (*12*) advanced an alternative theory for nest-site selection that is also consistent with the observed site fidelity of adult females. Under their social facilitation model, virgin (mature, unmated) females randomly encounter experienced females on foraging grounds. They then follow the experienced females to

A. B. Meylan, Department of Natural Resources, Florida Marine Research Institute, 100 Eighth Avenue, S.E., St. Petersburg, FL 33701, and Department of Herpetology and Ichthyology, American Museum of Natural History, New York, NY 10024.
B. W. Bowen and J. C. Avise, Department of Genetics, University of Georgia, Athens, GA 30602.